crystals

MDPI

Article

Interactions of Cr^{3+}, Ni^{2+}, and Sr^{2+} with Crushed Concrete Fines

Andrew P. Hurt [1], Aimee A. Coleman [2] and Nichola J. Coleman [1,*]

[1] School of Science, Faculty of Engineering and Science, University of Greenwich, Chatham Maritime, Kent ME4 4TB, UK; a.hurt@gre.ac.uk
[2] HH Wills Physics Laboratory, School of Physics, University of Bristol, Bristol BS8 1QU, UK; wy19042@bristol.ac.uk
* Correspondence: n.coleman@gre.ac.uk; Tel.: +44-208-331-9825

Abstract: The underutilized cement-rich fine fraction of concrete-based demolition waste is a potential sorbent for aqueous metal ion contaminants. In this study, crushed concrete fines (CCF) were found to exclude 33.9 mg g^{-1} of Cr^{3+}, 35.8 mg g^{-1} of Ni^{2+}, and 7.16 mg g^{-1} of Sr^{2+} from ~1000 ppm single metal nitrate solutions (CCF:solution 25 mg cm^{-3}) under static batch conditions at 20 °C after 3 weeks. The removal of Sr^{2+} followed a pseudo-second-order reaction ($k_2 = 3.1 \times 10^{-4}$ g mg^{-1} min^{-1}, $R^2 = 0.999$), whereas a pseudo-first-order model described the removal of Cr^{3+} ($k_1 = 2.3 \times 10^{-4}$ min^{-1}, $R^2 = 0.998$) and Ni^{2+} ($k_1 = 5.7 \times 10^{-4}$ min^{-1}, $R^2 = 0.991$). In all cases, the principal mechanism of interaction was the alkali-mediated precipitation of solubility-limiting phases on the surface of the CCF. Four consecutive deionized water leaching procedures (CCF:water 0.1 g cm^{-3}) liberated 0.53%, 0.88%, and 8.39% of the bound Cr^{3+}, Ni^{2+}, and Sr^{2+} species, respectively. These findings indicate that CCF are an effective sorbent for the immobilization and retention of aqueous Cr^{3+} and Ni^{2+} ions, although they are comparatively ineffectual in the removal and sustained exclusion of Sr^{2+} ions. As is commonly noted with Portland cement-based sorbents, slow removal kinetics, long equilibrium times, the associated release of Ca^{2+} ions, high pH, and the formation of loose floc may preclude these materials from conventional wastewater treatments. This notwithstanding, they are potentially suitable for incorporation into permeable reactive barriers for the containment of metal species in contaminated groundwaters, sediments, and soils.

Keywords: recycled; cement; concrete; demolition waste; chromium; nickel; strontium; heavy metals; sorbent

Citation: Hurt, A.P.; Coleman, A.A.; Coleman, N.J. Interactions of Cr^{3+}, Ni^{2+}, and Sr^{2+} with Crushed Concrete Fines. *Crystals* **2022**, *12*, 717. https://doi.org/10.3390/cryst12050717

Academic Editor: Chongchong Qi

Received: 29 April 2022
Accepted: 16 May 2022
Published: 18 May 2022

1. Introduction

Construction and demolition waste (C&DW) arising from the continual regeneration and expansion of urban environments accounts for approximately two-thirds of all global refuse [1]. Europe and China currently produce over 820 Mt and 1.8 Gt of C&DW per annum with respective recycling rates of 70% and 10% [2–5]. Over three-quarters of C&DW comprises concrete-based materials, from which the primary coarse aggregates can be recovered by crushing and grading for reuse in new concretes. The remaining low-density, alkaline, porous, cement-rich fine fraction is not effectively utilized.

The hydrated Portland cement component of concrete-based materials consists of a poorly crystalline calcium silicate hydrate (C-S-H) gel network (~70 wt%) interspersed with hexagonal calcium hydroxide crystals (~20 wt%) [6]. Various calcium aluminate hydrate phases (e.g., ettringite (AFt, $6CaO{\cdot}Al_2O_3{\cdot}3SO_3{\cdot}32H_2O$), monosulfate (AFm, $4CaO{\cdot}Al_2O_3{\cdot}SO_3{\cdot}13H_2O$), tetracalcium aluminate hydrate ($4CaO{\cdot}Al_2O_3{\cdot}13H_2O$), and hydrotalcite ($6MgO{\cdot}Al_2O_3{\cdot}CO_2{\cdot}12H_2O$)) are also dispersed throughout the cement matrix (depending on the composition and age of the cement) [6]. The nano- and micropores within the mature cement system contain residual mix water with dissolved Na^+, K^+, Mg^{2+}, Ca^{2+}, and OH^- ions that maintain the pH above 12.5. As the cement ages, the alkaline cement phases become progressively carbonated by exposure to atmospheric carbon dioxide.

For the past five decades, Portland cement-based systems have been a popular option for the stabilization and solidification of metal ions and radioisotopes in various contaminated liquids, sludges, ashes, soils, and sediments [7]. Metal ions and radionuclides can be immobilized within fresh Portland cement by isomorphic substitution into and sorption onto the hydration products, by complex formation, and by alkali-mediated precipitation of solubility-limiting phases [8]. In order to divert the large volumes of cement-rich C&DW from disposal by landfill, recent studies have been carried out to investigate the feasibility of using crushed concrete fines (CCF) to immobilize aqueous metal cations [9–19], oxyanions [5,16,20–24], and radioisotopes [25,26].

Chromium is known to exist at all oxidation states between −4 and +6, except −3, and is most commonly found in the environment as trivalent (Cr^{3+}) and hexavalent (CrO_4^{2-}) species [27]. In many countries (e.g., USA, Australia, New Zealand, and Japan), trivalent chromium is regarded as an essential dietary element for carbohydrate and lipid metabolism; although, in 2014, the European Food Safety Agency concluded that chromium is not essential for humans [28]. No adverse toxicological effects are attributed to trivalent chromium in humans, owing to its poor cell membrane permeability, although it can cause DNA damage and is associated with toxicity in aquatic organisms [29]. Trivalent chromium compounds are widely used in tanning, paints, inks, pigments, catalysts, and electroplating. Effluents arising from these industries are limited to a maximum discharge of 5 ppm for total chromium in the EU [27].

Aqueous Cr^{3+} ions are reported to be immobilized in fresh cement paste via substitution for Si^{4+} in C-S-H gel and by replacement of octahedral Al^{3+} in calcium aluminate hydrate phases [8,30]. A previous batch study has also indicated that 10 g of CCF can remove 96% of Cr^{3+} ions from 100 cm^3 of 100 ppm single metal nitrate solution within 24 h, although the fate of the adsorbed ions was not reported [31].

The redox chemistry of nickel encompasses all oxidation states between −2 and +4, with divalent nickel (Ni^{2+}) being the most prevalent species in biology and the environment [32]. Nickel is essential for some microorganisms, plants, and animals and is present in the human diet via various fruits, vegetables, grains, and seafood [32]. There is no evidence that nickel is directly essential to humans, although it may be required by certain gut bacteria. Skin exposure to nickel can cause contact dermatitis, and chronic inhalation is associated with asthma, lung fibrosis, and respiratory tract cancers. Nickel is used in the manufacture of metal alloys, electroplating, batteries, and catalysts. The ^{63}Ni radionuclide is used in surge protectors and betavoltaic devices and is a common constituent of liquid waste arising from nuclear plant decommissioning [17–19].

Multiple immobilization mechanisms have been proposed for Ni^{2+} ions in fresh cement pastes [8]. These include substitution for Ca^{2+} in ettringite, complexation with silanol (-Si-OH) groups of C-S-H gel, coprecipitation with Ca^{2+} as hydroxides, and the formation of mixed Ni-Al layered double hydroxides [8]. Shin et al. [9] reported that mature laboratory CCF pre-treated with sodium hydroxide solution adsorbed 0.531 mg g^{-1} of Ni^{2+} under batch conditions from a 10 ppm solution at a solid:solution ratio of 1.0 mg cm^{-3} within 6 h. A considerably higher adsorption capacity of 31.7 mg g^{-1} was reported for Ni^{2+} uptake by 50-year-old demolition CCF (at a solid:solution ratio of 5 mg cm^{-3} from 470 ppm solution within 24 h) [19]. Neither study addressed the removal mechanism(s) of Ni^{2+} by CCF [9,19].

The general, biological and environmental chemistry of strontium is dominated by the +2 oxidation state, although molecular strontium(I) halides can be formed in the gas phase [33]. Strontium is substituted for calcium in the mineralized hydroxycarbonate apatite component of human bone, where it can exert either beneficial or deleterious effects depending on concentration [34]. Strontium was formerly used in cathode ray tubes and still finds application in fireworks, flares, glow-in-the-dark paints, toothpaste, ferrite magnets, and zinc refinery [35]. The ^{90}Sr radioisotope is a significant component of spent nuclear fuels and weapons fallout, and it is also used in thermoelectric generators, gauges,

and radiotherapy [17–19]. ^{90}Sr accumulates in bone and bone marrow, causing cancers in the host tissue, surrounding soft tissues, and blood.

Weiland et al. [26] found that the principal immobilization mode of Sr^{2+} ions by hardened sulfate-resisting Portland cement was the binding of partially hydrated Sr^{2+} species to C-S-H gel via bridging oxygen atoms. At low Sr^{2+} concentration (0.175 ppb in 'artificial cement water'), the controlling mechanism was determined to be ion-exchange of Sr^{2+} for Ca^{2+} ions. A subsequent study on the interactions of 88 ppm aqueous Sr^{2+} ions with individual cement phases (C-S-H, AFt, AFm, and $3CaO{\cdot}Al_2O_3{\cdot}6H_2O$) indicated that Sr^{2+} displaces Ca^{2+} from C-S-H gel and also from the calcium aluminate hydrate phases [36]. Subsequent desorption analysis of Sr^{2+} from the C-S-H gel phase additionally revealed multiple surface sorption processes (that were not specified) [36].

Mature CCF from the demolition of a 1970s concrete pavement were recently found to have a maximum Sr^{2+} removal capacity of 21.9 mg g^{-1} (from 700 ppm nitrate solution, at solid:solution ratio 5 mg cm^{-3}, after 24 h at ambient temperature) [19]. The removal mechanisms were reported to be a combination of electrostatic adsorption and the precipitation of acid-soluble species such as carbonates [19].

The present study considered the interactions of aqueous Cr^{3+}, Ni^{2+}, and Sr^{2+} ions with the 1–2 mm fraction of CCF under single metal batch conditions. The metal ion removal profiles were analyzed using the pseudo-first- and pseudo-second-order kinetic models. The nature of the CCF-bound metal species was investigated by scanning electron microscopy (SEM) and energy-dispersive X-ray spectroscopy (EDX), and a deionized water leaching procedure was used to determine the reversibility of binding. The experimental component of this research was based upon previous studies to investigate the interactions of aqueous Cu^{2+}, Zn^{2+}, Pb^{2+}, Cd^{2+}, Co^{2+}, and MoO_4^{2-} with CCF [12,37].

2. Materials and Methods

2.1. Prepraration and Characterization of Crushed Concrete Fines (CCF)

The 1–2 mm CCF used in this study, which was carried out in 2004, were obtained by jaw-crushing and sieving a 5-year-old concrete block prepared from ordinary Portland cement (OPC) and sea-dredged flint aggregate at a water:cement ratio of 0.4. The constituent phases of the cement were determined, by differential thermal analysis, to be C-S-H gel, portlandite, ettringite, tetracalcium aluminate hydrate, and calcite, which are typical components of mature hydrated OPC [12]. The cement content of the CCF granules was determined by nitric acid digestion [12]. The mix proportions of the concrete block and the cement content of the CCF are listed in Table 1.

Table 1. Mix proportions of concrete block and cement contents of the block and CCF.

Constituent	Mass (kg)	Cement Content (%)
OPC	28.32	-
Water	11.37	-
5 mm aggregate	13.90	-
10 mm aggregate	44.22	-
20 mm aggregate	43.87	-
Cement content of block	-	~28
Cement content of CCF	-	50.1 ± 0.4

2.2. Uptake of Aqueous Cr^{3+}, Ni^{2+}, and Sr^{2+} Ions by CCF

The removal of Cr^{3+}, Ni^{2+}, and Sr^{2+} ions by CCF from aqueous single metal ion solutions of $Cr(NO_3)_3{\cdot}9H_2O$, $Ni(NO_3)_2{\cdot}6H_2O$, and $Sr(NO_3)_2$, respectively, were carried out in triplicate under static batch conditions. For each analysis, 2.5 g of CCF were contacted with 100 cm^3 of ~1000 ppm single metal nitrate solution or deionized water (control) in a screw-capped polypropylene container at 20 °C. The actual Cr^{3+}, Ni^{2+}, and Sr^{2+} ion concentrations were 850 ± 8 ppm, 900 ± 12 ppm, and 991 ± 5 ppm, respectively. Aliquots of the supernatant liquors (0.5 cm^3) were withdrawn at various times between 3 h and

120 h for elemental analysis by inductively coupled plasma optical emission spectroscopy (ICP-OES) using a TJA Iris simultaneous ICP-OES spectrometer (TJA, Waltham, MA, USA). The relative standard deviations were within 8%, 6%, and 7% of the mean concentration values for Cr^{3+}, Ni^{2+}, and Sr^{2+}, respectively.

Metal ion removal data were analyzed using the pseudo-first- and pseudo-second-order kinetic models [37,38]. The linear form of the pseudo-first-order rate equation, that describes processes in which the reaction rate is proportional to the number of available sorption sites, is given by the following equation [37,38]:

$$\log (q_e - q_t) = \log q_e - k_1 t/2.303 \quad (1)$$

where k_1 (in min^{-1}) is the apparent pseudo-first-order rate constant, q_t (in mg g^{-1}) is the extent of sorption at time t (in min), and q_e (in mg g^{-1}) is the extent of sorption at equilibrium. This rate equation applies when a linear relationship exists between $\log(q_e - q_t)$ and t, in which case k_1 can be estimated from the gradient of the plot.

The pseudo-second-order rate equation describes sorption processes in which the reaction rate is proportional to the square of the number of available sorption sites and is represented, in linear form, as follows [37,38]:

$$t/q_t = 1/k_2 {q_e}^2 + t/q_e \quad (2)$$

where k_2 (in g mg^{-1} min^{-1}) is the apparent pseudo-second-order rate constant. Estimates of k_2 and q_e can be obtained from the intercept and gradient of a linear plot of t/q_t against t.

2.3. Leaching of Cr^{3+}, Ni^{2+}, and Sr^{2+} Ions from Metal-Bearing CCF

To evaluate the binding and subsequent leaching of the metal ions, additional batch sorption experiments were carried out, as outlined in Section 2.2, in which 2.5 g of CCF were placed in contact with 100 cm^3 of ~1000 ppm single metal ion solution for 3 weeks. The metal-bearing CCF granules were then retrieved in a 0.5 mm mesh polypropylene sieve, rinsed twice with 50 cm^3 of deionized water to remove loose precipitate, and dried in air at 20 °C to constant mass.

The recovered metal-bearing CCF samples were subjected to a 24 h deionized water leaching procedure, which was carried out in triplicate, at room temperature, at a solid:solution ratio of 0.1 g cm^{-3}, and repeated four consecutive times [12]. The leachates were analyzed for the relevant metals by ICP-OES.

Triplicate sub-samples of the recovered metal-bearing CCF were also digested in concentrated nitric acid, and the resulting liquors were analyzed by ICP-OES for the relevant heavy metal. The proportions of metal species bound to CCF, present in solution and as loose precipitate, were then calculated via a mass balance for each metal.

2.4. Characterization of Metal-Bearing CCF by SEM and EDX

Secondary electron images of the surfaces of gold-coated CCF samples prior to and following immersion in ~1000 ppm metal solutions for 3 weeks were acquired using a JEOL JSM-5310LV scanning electron microscope (JEOL (UK) Ltd., Welwyn Garden City, UK) at an accelerating voltage of 20 kV in high-vacuum mode. Carbon-coated CCF surfaces and polished cross-sections were analyzed by EDX using an Oxford Instruments Isis 300 X-ray microanalysis system (Oxford Instruments, Abingdon, UK) at a working distance of 20 mm. EDX maps of Ca, Si, Cr, and Ni were obtained using characteristic Kα X-ray lines, and the Lα X-ray line was used for the EDX mapping of Sr.

3. Results

3.1. Removal of Cr^{3+}, Ni^{2+}, and Sr^{2+} Ions by CCF

The removal profiles of Cr^{3+}, Ni^{2+}, and Sr^{2+} ions from single metal nitrate solutions by CCF under batch conditions are plotted in Figure 1, and the corresponding pH values of

the supernatant liquors are shown in Figure 2. The removal of Cr^{3+} ions increased steadily throughout the 5-day observation period to a maximum value of 31.1 ± 0.6 mg g^{-1}, which corresponded with a removal efficiency of 91.2% (Figure 1). A concomitant increase in supernatant pH from 2.7 to 6.0 accompanied the removal of Cr^{3+} ions from the solution (Figure 2). A maximum exclusion of 35.9 ± 0.7 mg g^{-1} (i.e., 99.7%) was observed for Ni^{2+} ions in the presence of CCF after 5 days (Figure 1), with an associated increase in pH from 6.5 to 9.6 (Figure 2). Equilibrium Sr^{2+} removal of 7.00 ± 0.15 mg g^{-1} (i.e., 17.7%) was achieved within 3 days (Figure 1), with an accompanying increase in pH from 6.7 to 11.5 that differed insignificantly from the control system in which CCF were contacted with deionized water (Figure 2).

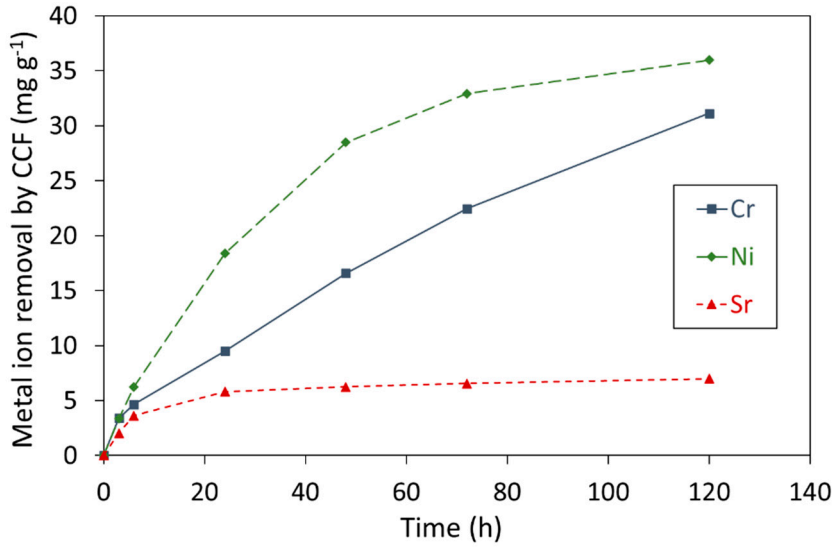

Figure 1. Removal of aqueous Cr^{3+}, Ni^{2+}, and Sr^{2+} ions by CCF.

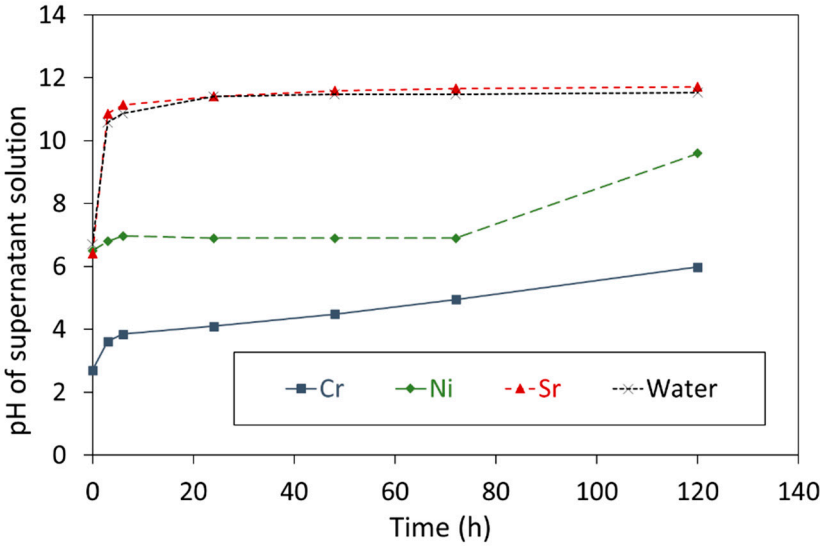

Figure 2. pH of deionized water and aqueous solutions of Cr^{3+}, Ni^{2+}, and Sr^{2+} in contact with CCF.

Data for the removal of Cr^{3+}, Ni^{2+}, and Sr^{2+} by CCF were fitted to the pseudo-first- and pseudo-second-order rate models [37,38] for which the apparent rate constants, k_1 and k_2, the calculated equilibrium removal values, $q_{e\ calc.}$, and the respective squares of the linear regression coefficients, R^2, are listed in Table 2. The removal of Cr^{3+} and Ni^{2+} ions were found to follow pseudo-first-order kinetics, and Sr^{2+} removal was better described by the pseudo-second-order reaction rate (Table 2).

Table 2. Kinetic parameters for the removal of Cr^{3+}, Ni^{2+}, and Sr^{2+} from aqueous solution by CCF.

Kinetic Parameter	Cr	Ni	Sr
Pseudo-first-order model			
k_1 (min^{-1})	2.3×10^{-4}	5.7×10^{-4}	4.9×10^{-4}
$q_{e\ calc.}$ (mg g^{-1})	32.7	37.3	4.14
R^2	0.991	0.998	0.945
Pseudo-second-order model			
k_2 (g mg^{-1} min^{-1})	1.0×10^{-5}	1.4×10^{-5}	3.1×10^{-4}
$q_{e\ calc.}$ (mg g^{-1})	40.3	46.7	7.36
R^2	0.877	0.996	0.999

The extents of Cr^{3+}, Ni^{2+}, and Sr^{2+} removal, and the concentrations of soluble calcium, aluminum, and silicate species released from the CCF after 3 weeks, are listed in Table 3. These data confirm that the exclusion of Cr^{3+} increased modestly from 31.1 mg g^{-1} to 33.9 mg g^{-1} between 5 days (Figure 1) and 3 weeks (Table 3) and that no further removal of either Ni^{2+} or Sr^{2+} occurred within this timeframe. The calculated equilibrium extents of exclusion of Cr^{3+} and Ni^{2+} ions derived from the pseudo-first-order model (Table 2) were, respectively, within 3.5% and 4.2% of the observed experimental values (Table 3). Additionally, the experimental equilibrium removal of Sr^{2+} ions (Table 3) agreed with the value calculated from the pseudo-second-order model (Table 2) to within 2.8%.

Table 3. Metal ion removal and dissolution of major constituents of CCF after 3 weeks.

Property	Control	Cr	Ni	Sr
Metal ion removal (mg g^{-1})	-	33.9 ± 1.2	35.8 ± 1.1	7.16 ± 0.31
Calcium dissolution (mg g^{-1})	7.42 ± 0.32	42.8 ± 1.7	29.2 ± 0.9	12.1 ± 0.5
Aluminum dissolution (mg g^{-1})	0.13 ± 0.01	b.d.l.	b.d.l.	0.13 ± 0.01
Silicon dissolution (mg g^{-1})	0.18 ± 0.02	0.08 ± 0.03	0.03 ± 0.02	0.14 ± 0.02

b.d.l. = below detection limit.

The release of calcium ions from CCF in deionized water (7.42 mg g^{-1}), arising from the dissolution of calcium hydroxide, was significantly lower than that in each of the metal ion solutions (Table 3). This indicates that additional calcium ions are released from CCF to maintain charge neutrality as the metal ions are sequestered from the solution. Conversely, the extents of dissolution of silicate and aluminum species from CCF in the deionized water control are greater than those observed in the presence of Cr^{3+} and Ni^{2+} ions (Table 3), which suggests that these species may be involved in the metal ion immobilization process.

The uptake of Cr^{3+} (28.6 mg g^{-1}), Ni^{2+} (28.7 mg g^{-1}), and Sr^{2+} (3.77 mg g^{-1}) by binding to CCF after 3 weeks was determined by nitric acid digestion. The corresponding quantities of Cr^{3+}, Ni^{2+}, and Sr^{2+} present in the loose floc precipitate that also formed on prolonged exposure to CCF were then estimated by a mass balance for each metal ion. The distribution of each metal species among the solution, floc, and CCF particles is shown in Figure 3. Greater than 99% of the initial concentrations of Cr^{3+} and Ni^{2+} ions were excluded from the solution after 3 weeks, with 84% and 80%, respectively, bound to the CCF (Figure 3). The removal efficiency of CCF for Sr^{2+} was considerably lower, with 82% remaining in solution and only 9.5% sequestered by the CCF (Figure 3).

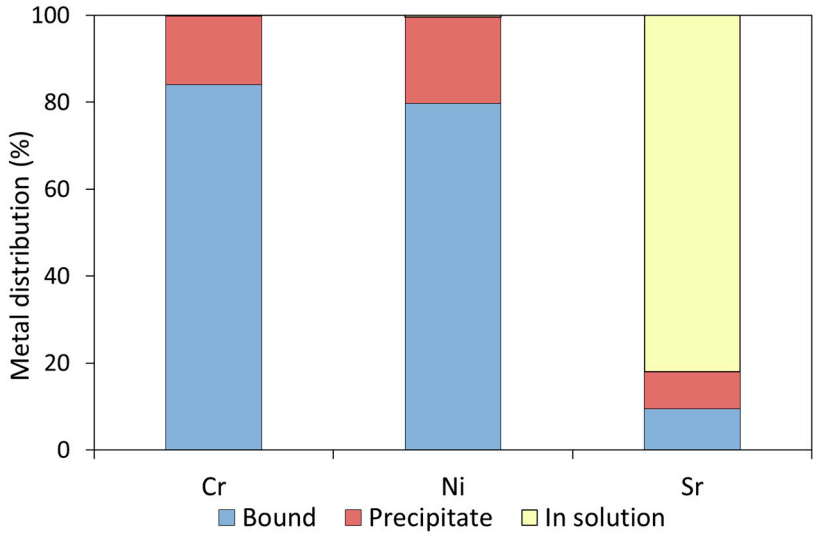

Figure 3. The distribution of each metal species in contact with CCF for 3 weeks.

3.2. Leaching of Cr^{3+}, Ni^{2+}, and Sr^{2+} Species Bound to CCF

The cumulative concentrations of the Cr^{3+}, Ni^{2+}, and Sr^{2+} ions leached from CCF during four consecutive deionized water leach tests are plotted in Figure 4. These data demonstrate that the maximum proportions of heavy metals leached were Cr^{3+} (0.52%) < Ni^{2+} (0.88%) < Sr^{2+} (8.4%). The extent of dissolution of Cr^{3+} and Ni^{2+} species markedly diminished with each consecutive leaching procedure, whereas the rate of release of Sr^{2+} ions was approximately constant at 0.075 mg g^{-1} per test (Figure 4).

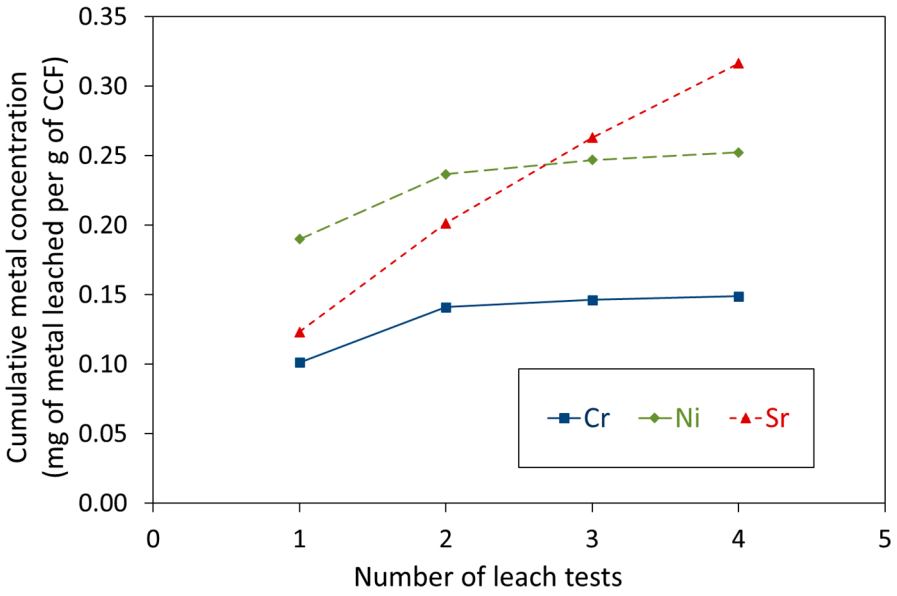

Figure 4. Cumulative concentration of metal species in deionized water leachate.

3.3. The Fate of Metal Species Bound to CCF

A photographic image of the recovered CCF following exposure to the chromium(III), nickel(II), and strontium(II) nitrate solutions for 3 weeks is shown in Figure 5. The uptake of Cr^{3+} by the cement component is evidenced in sample CCF-Cr by its characteristic dark violet color, and likewise, CCF-Ni is pigmented with light green Ni^{2+} ions (Figure 5). Since Sr^{2+} ions are colorless, CCF-Sr is visually indistinguishable from the original CCF comprising gray hydrated cement grains. In each sample, the fine flint aggregate that accounts for ~50 wt% of the CCF is visible as brown, beige, and yellow granules.

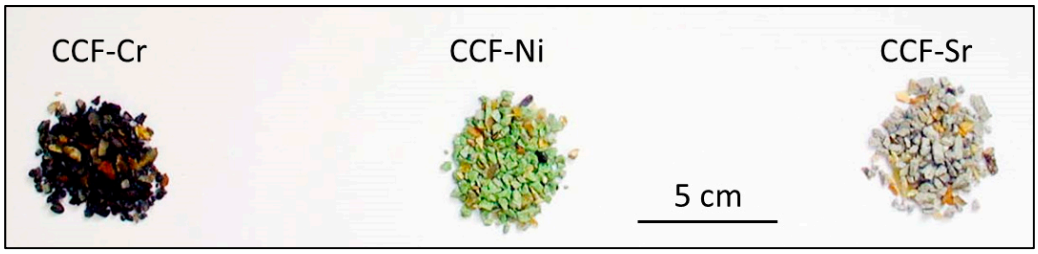

Figure 5. Photographic image of CCF-Cr, CCF-Ni, and CCF-Sr.

Secondary electron images of the surfaces of CCF prior to and following the 3-week immersion period in Cr^{3+}, Ni^{2+}, or Sr^{2+} solution are presented in Figure 6. The relative aluminum, silicon, calcium, and metal ion concentrations of the precipitates formed on the surfaces of CCF on exposure to the metal-bearing solutions are listed in Table 4.

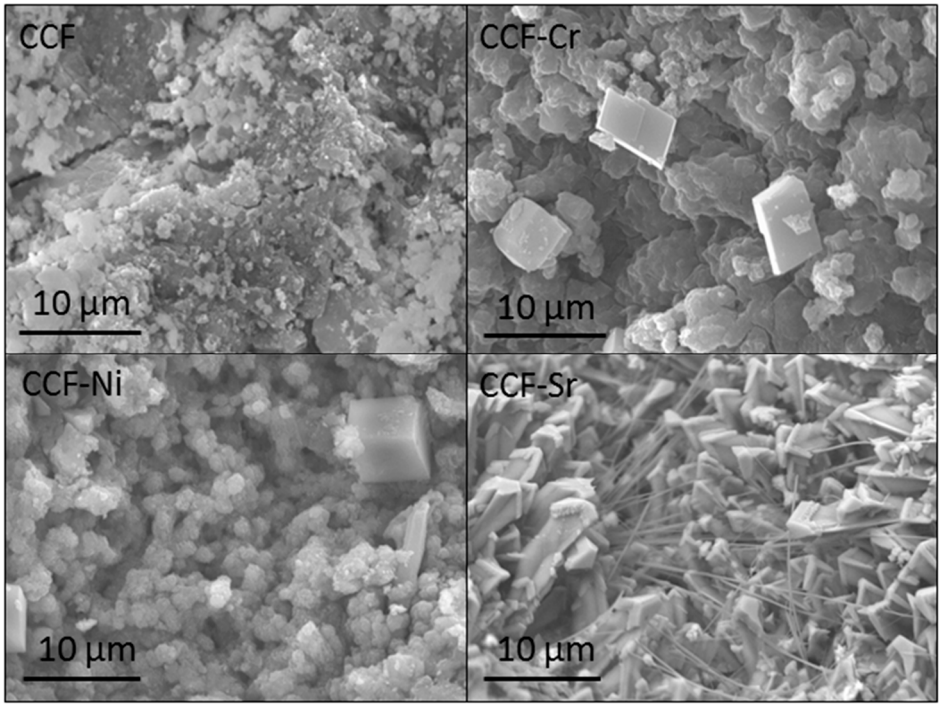

Figure 6. Secondary electron images (×3500) of the surfaces of crushed concrete fines (CCF), chromium-bearing CCF (CCF-Cr) depicting occasional rhomboids over layered platy deposits, nickel-bearing CCF (CCF-Ni) showing occasional cubes over a colloform network, and strontium-bearing CCF (CCF-Sr) portraying thread-like structures over clusters of spear-headed fronds.

Table 4. Compositions of metal-bearing structures on the surface of CCF (determined by EDX).

Structure	Relative Elemental Composition (Moles per Mole of Al) [1]			
	Al	Si	Ca	Metal Ion
CCF-Cr				
Platy deposits	1.00 ± 0.45	4.07 ± 2.33	33.8 ± 3.2	117 ± 10
Rhomboids	1.00 ± 0.25	3.35 ± 0.67	201 ± 19	24.0 ± 8.5
CCF-Ni				
Colloform network	1.00 ± 0.37	2.48 ± 0.65	1.38 ± 0.37	28.7 ± 0.76
Cubes	1.00 ± 0.47	1.40 ± 0.26	239 ± 9.8	9.45 ± 3.1
CCF-Sr				
Spear-headed fronds	1.00 ± 0.31	4.79 ± 0.72	168 ± 3.9	22.2 ± 1.8

[1] All data are normalized to the proportion of aluminum present.

The hydrated cement granules of CCF presented irregular textured surfaces at the micron scale that are typical of mechanically crushed concrete [37] (Figure 6). The surface of CCF-Cr was characterized by a layered platy deposit (Cr:Ca = 3.46:1.00) scattered with occasional rhomboids (Cr:Ca = 1.00:8.38) (Figure 6). The back-scattered electron micrograph and accompanying EDX maps for Cr, Ca, and Si through a cross-section of a CCF-Cr particle are shown in Figure 7. These images demonstrate that the mechanism of interaction of Cr^{3+} with CCF was the initial formation of a 40 μm Cr-rich platy deposit and the subsequent precipitation of Ca-rich mixed-metal hydroxide crystals. The Cr-bearing phases were observed to have exclusively precipitated onto the surface of the cement granules with no evidence of Cr^{3+} diffusion into the cement matrix (Figure 7).

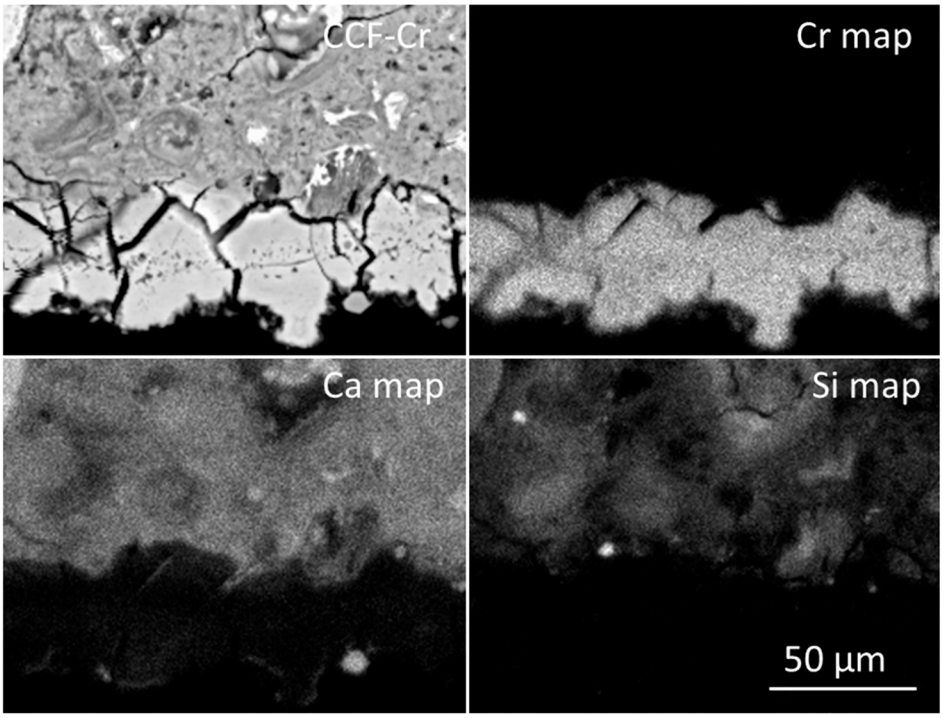

Figure 7. Back-scattered electron micrograph of cross-section of chromium-bearing CCF particle and corresponding EDX maps for chromium, calcium, and silicon.

The surface of CCF-Ni was found to be populated with rare cubic structures (Ni:Ca = 1.00:25.3) deposited over a colloform network (Ni:Ca = 20.8:1.00) (Figure 6). The back-scattered electron image of a cross-section through a CCF-Ni particle and corresponding EDX maps of Ni, Ca, and Si are presented in Figure 8. These data indicate that the mechanism of uptake of Ni^{2+} by CCF, which was similar to that of Cr^{3+}, involved the initial deposition of a 40 μm Ni-rich precipitate with the subsequent formation of Ca-rich mixed-metal hydroxide crystals (Figure 8).

The CCF-Sr surface presented fine thread-like structures over discrete clusters of spear-headed fronds (Sr:Ca = 1.00:7.57) (Figure 6). The back-scattered electron micrograph of a cross-section through a CCF-Sr particle (Figure 9) shows the Sr-bearing precipitates (<10 μm) dispersed non-contiguously across the surface. Interference occurs from the overlap of the Si Kα line (1.740 keV) with the Sr Lα line (1.806 keV) to give the impression of a low concentration of Sr^{2+} species homogeneously distributed within the interior of the cement matrix (as indicated by the EDX Sr map in Figure 9). This background signal arises from interference from the silicon present in C-S-H and not from any appreciable diffusion of Sr^{2+} ions within the interior of the cement particle (which would have given rise to a graduated signal intensity).

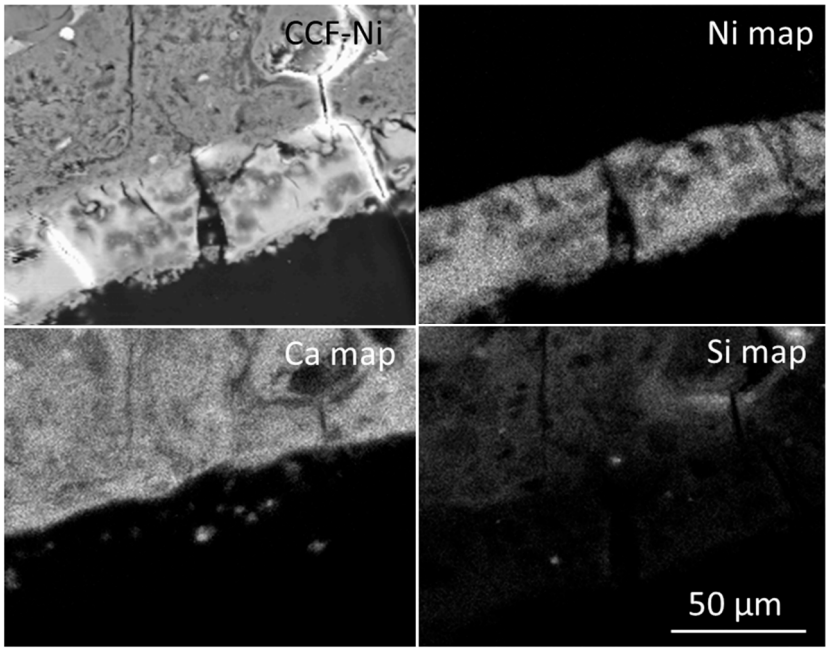

Figure 8. Back-scattered electron micrograph of cross-section of nickel-bearing CCF particle and corresponding EDX maps for nickel, calcium, and silicon.

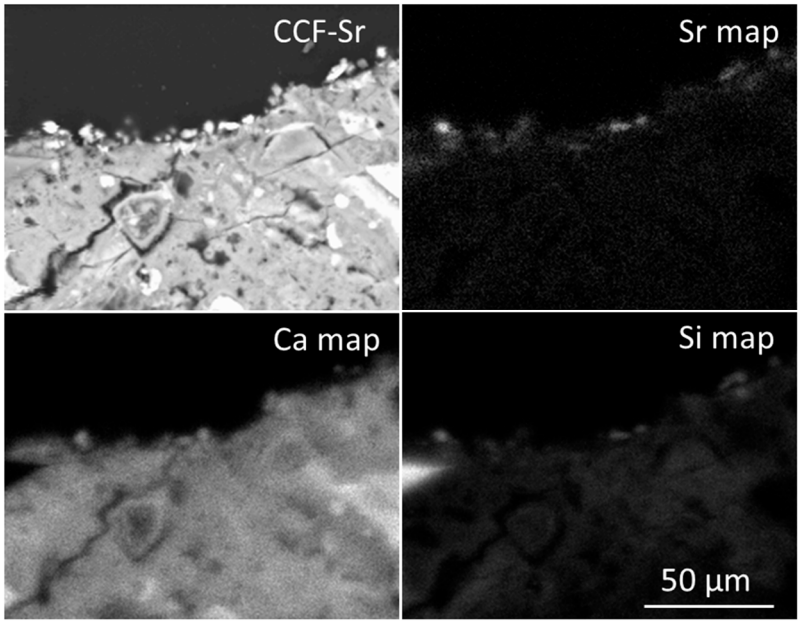

Figure 9. Back-scattered electron micrograph of cross-section of strontium-bearing CCF particle and corresponding EDX maps for strontium, calcium, and silicon.

4. Discussion

The 1–2 mm crushed concrete fines used in this study were shown to remove 33.9 mg g^{-1} of Cr^{3+}, 35.8 mg g^{-1} of Ni^{2+}, and 7.16 mg g^{-1} of Sr^{2+} from ~1000 ppm single-metal nitrate solutions under static batch conditions at 20 °C after 3 weeks. The sequestration of Cr^{3+} and Ni^{2+} ions took place via the alkali-mediated precipitation of a metal-rich layer bound directly to the surface of the cement granules, which was then followed by the precipitation of discrete Ca-rich mixed-metal hydroxide crystals (Figures 6–8). The inferior removal of Sr^{2+} by CCF was attributed to the inability of the Sr^{2+} ion to form solubility-limiting oxides and hydroxides at elevated pH, and the principal mechanism of immobilization of Sr^{2+}

appeared to be its incorporation into a Ca-rich precipitate. All three metal ions, Cr^{3+}, Ni^{2+}, and Sr^{2+}, are known to substitute into hydrated cement phases [8,26,30,36], although no appreciable diffusion into the cement matrix was observed under the selected experimental conditions in this study.

On exposure to deionized water, CCF readily released calcium, alkali metal, and hydroxide ions from the pore fluid, which increased the supernatant pH to 10.6 within 3 h (Figure 2). Subsequent ion release and the dissolution of portlandite further elevated the pH to a steady-state value of 11.5 after 24 h. The pH profile of the Sr^{2+}-bearing supernatant liquor in contact with CCF differed insignificantly from that of the deionized water control, as the solubility and speciation of Sr^{2+} ions are little affected by pH (Figure 2). Conversely, more modest elevations in supernatant pH were observed for the Cr^{3+}- and Ni^{2+}-bearing solutions in contact with CCF, as the released hydroxide ions were directly engaged in the precipitation of these metals (Figure 2).

A previous study indicated that there may be a linear relationship between the uptake of divalent metal cations and the concomitant dissolution of Ca^{2+} ions from CCF [12]. To test this postulate, equilibrium data from the present and two previous studies [12,37] were collated to plot the total charge of dissolved Ca^{2+} ions against the total charge of metal ions removed by CCF (Figure 10). Regression analysis (R^2 = 0.9895) confirmed the linearly proportional release of Ca^{2+} ions as a function of metal ion immobilization (Figure 10) irrespective of the charge of the metal cation or the nature of its interaction with the CCF. It should be noted that Sr^{2+}, Cd^{2+}, Zn^{2+}, Cu^{2+}, Ni^{2+}, and Cr^{3+} are all reported to form solubility-limiting precipitates in contact with CCF, whereas Pb^{2+} diffuses into the cement matrix to replace Ca^{2+} within the hydrated phases [12,37]. Hence, the release of Ca^{2+} ions in contact with CCF is potentially predictable for the sequestration of metal cations and is independent of the specific immobilization mechanisms.

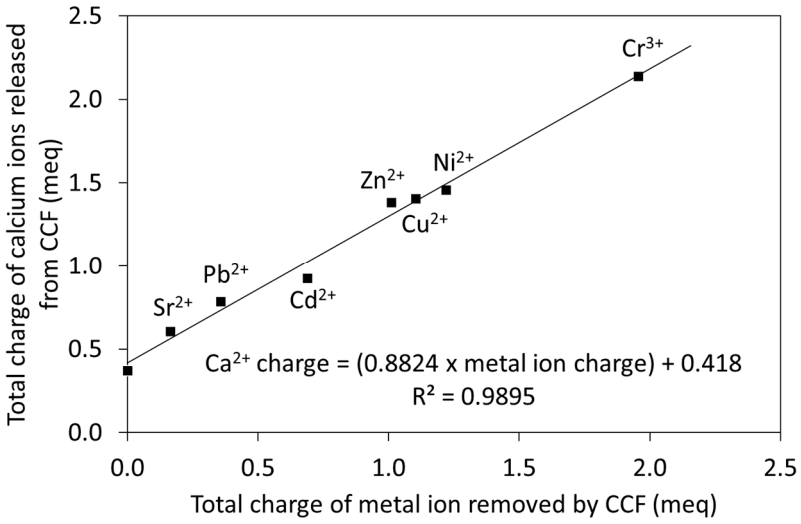

Figure 10. The charge of Ca^{2+} ions released by CCF plotted as a function of the charge of the metal ion removed by CCF for Cr^{3+}, Ni^{2+}, and Sr^{2+} reported in the present study, Pb^{2+} [12], Zn^{2+} [12], Cu^{2+} [12], and Cd^{2+} [37].

In the present study, the pseudo-first-order kinetic model accurately described the removal of Cr^{3+} ($k_1 = 2.3 \times 10^{-4}$ min^{-1}, R^2 = 0.998) and Ni^{2+} ($k_1 = 5.7 \times 10^{-4}$ min^{-1}, R^2 = 0.991) by CCF and predicted the equilibrium uptakes to within 3.5% and 4.2%, respectively (Table 2). The removal of Sr^{2+} was found to follow a pseudo-second-order reaction ($k_2 = 3.1 \times 10^{-4}$ g mg^{-1} min^{-1}, R^2 = 0.999) with 2.8% agreement between the experimental and calculated values for equilibrium removal (Table 2). The pseudo-first- and pseudo-second-order kinetic models used in this study have been widely applied to describe the sorption of aqueous contaminants by a variety of solid-state materials [37–40].

The pseudo-first-order kinetic model is often reported to denote physisorption, whereas the pseudo-second-order kinetic model is generally considered to signify that the rate-limiting step involves chemisorption. However, the relationship between these pseudo kinetic models and the specific sorption mechanisms is contentious. One theoretical argument suggests that the applicability of these kinetic models arises from the initial solute concentration rather than a specific sorption mechanism [38]. High solute concentrations are demonstrated to conform to apparent pseudo-first-order kinetics, and pseudo-second-order kinetics become more relevant as the initial solute concentration decreases. Similarly, it has also been proposed that the pseudo-first-order model provides an adequate description of many systems for an initial period and that the pseudo-second-order model affords a better long-term forecast [40]. It is clear that these pseudo kinetic models do not reveal information regarding the mechanism of metal ion uptake by CCF; nonetheless, they provide a potentially reliable tool for comparison and prediction.

The steady-state removal capacities and equilibrium times observed in this study are compared with those of other waste concretes and low-cost silicate-based sorbents in Table 5 [9,19,25,41–49]. The removal capacity of CCF for Cr^{3+} was within the reported range of other candidate sorbents, although the equilibrium time, greater than 5 days, was markedly longer than that of any other material (Table 5). Maximum Ni^{2+} removal by CCF was superior to that of waste ceramic tiles [47] and compared favorably with the values obtained for other crushed concretes [9,19,46] (Table 5). The removal efficiency and equilibrium time observed in this study for the interaction of Sr^{2+} with CCF are intermediate between those reported for other laboratory [25] and demolition [19] CCF (Table 5). The comparatively high Sr^{2+} removal capacity reported by Jelić et al. (21.9 mg g^{-1}) [19] is, in all probability, attributed to the use of 50-year-old demolition concrete, which had been subjected to extensive atmospheric carbonation. In that study, sequential extraction of the Sr^{2+}-laden demolition CCF indirectly indicated that the majority of the Sr^{2+} ions were precipitated as acid-soluble species such as carbonates [19]. As previously mentioned, Sr^{2+} does not form alkali-mediated solubility-limiting oxides and hydroxides, although strontium carbonate is highly insoluble at neutral and alkaline pH ($K_{sp} = 5.6 \times 10^{-10}$) [50]. The comparatively low Sr^{2+} removal capacity (0.675 mg g^{-1}) reported by Kitternova et al. [25] is considered to have arisen from the limited extent of carbonation of the relatively young (<3 years) laboratory CCF.

Table 5. Comparison of the removal of Cr^{3+}, Ni^{2+}, and Sr^{2+} by CCF with those of other waste concretes and silicate-based inorganic sorbents.

Sorbent	[1] C_i Range (ppm)	Solid:Liquid Ratio (mg cm^{-3})	[2] q_m (mg g^{-1})	[3] t_{eq} (min)	Ref
Chromium, Cr^{3+}					
Laboratory CCF	850	25	33.9	>7200	This study
Geopolymer	50–300	0.001–0.02	19.9	4320	[41]
Waste-derived tobermorite	520–2600	7	253	360	[42]
Calcium silicate hydrate	1000	10	100	300	[43]
Bentonitic clay	10–300	0.5–6	117.5	60	[44]
Fly ash-derived zeolite A	100	25	4.0	30	[45]
Nickel, Ni^{2+}					
Laboratory CCF	900	25	35.8	7200	This study
Demolition CCF	5.87–470	5	31.7	1440	[19]
Demolition CCF	100–750	50–3000	13.6	300	[46]
NaOH-pretreated CCF	10	1	0.531	360	[9]
Waste-derived calcium silicate	200	2.5	79.2	180	[39]
Waste ceramic tiles	5.87–470	5	7.04	3000	[47]

Table 5. *Cont.*

Sorbent	[1] C_i Range (ppm)	Solid:Liquid Ratio (mg cm^{-3})	[2] q_m (mg g^{-1})	[3] t_{eq} (min)	Ref
Strontium, Sr^{2+}					
Laboratory CCF	991	25	7.16	4320	This study
Laboratory CCF	0–30.7	0.0017–0.1	0.675	5760	[25]
Demolition CCF	8.76–701	5	21.9	1440	[19]
Waste-derived tobermorite	0–100	50	1.52	7200	[48]
Waste ceramic tiles	8.76–701	5	3.07	1500	[47]
Alkali-activated metakaolin	10–3000	10	180	240	[49]

[1] C_i = initial metal concentration in solution. [2] q_m = maximum metal uptake. [3] t_{eq} = time to equilibrium.

One general observation is that metal ion sequestration by exchange for labile calcium or sodium ions in crystalline calcium silicate minerals (e.g., tobermorite [42], dibasic calcium silicate hydrate [43], layered clay [44], and zeolite A [45]) tends to reach equilibrium within minutes or hours, rather than several days, which is the case for the precipitation of solubility-limiting phases on CCF (Table 5).

The slow removal kinetics, associated release of Ca^{2+} ions, high pH, and the formation of loose floc are likely to preclude the use of CCF from conventional wastewater treatments. However, they are potentially suitable for incorporation into permeable reactive barriers (PRBs) for the management of acidity and containment of metal species in contaminated groundwaters, sediments, and soils. Metal-contaminated acidic soil and groundwater is a widespread problem arising from mining, land reclamation, large-scale drainage, and agriculture [51]. Adverse ecological and environmental effects are exacerbated by the fact that toxic metal species tend to be highly soluble and mobile under acidic conditions. The use of CCF in PRBs could favorably exploit both the acid neutralization capacity of the cement (i.e., the release of hydroxide ions to elevate the groundwater pH) and its ability to sequester metal species via the formation of solubility-limiting phases. In this respect, laboratory and pilot-scale studies have been carried out to determine the performance of crushed demolition concrete in PRBs to manage acid sulfate soils and groundwaters in the coastal floodplains of Australia [51–54]. The possibility of rejuvenating crushed concrete in situ with alkaline wastewater is also being explored to improve the performance and extend the lifespan of PRBs [53]. The replacement of geological materials, such as limestone and zeolites, with CCF in PRBs not only utilizes a problematic waste but also contributes to the conservation of natural mineral resources.

5. Conclusions

This study demonstrated that crushed concrete fines (CCF) are highly effective in the sequestration of Cr^{3+} (33.9 mg g^{-1}) and Ni^{2+} (35.8 mg g^{-1}) from aqueous solution, with a significantly lower removal capacity for Sr^{2+} (7.16 mg g^{-1}). The mechanism of removal was found to be the alkali-mediated formation of solubility-limiting phases bound to the surface of the cement particles, which was also accompanied by the precipitation of loose floc. Approximately 8% of the sorbed Sr^{2+} ions were released in four consecutive deionized water leaching tests, and less than 1% of the bound Cr^{3+} and Ni^{2+} species were readily leachable. These findings indicate that CCF are an effective sorbent for the removal and retention of aqueous Cr^{3+} and Ni^{2+} ions, although they are comparatively ineffectual in the uptake and sustained exclusion of Sr^{2+} ions. Slow removal kinetics, the concomitant release of Ca^{2+} ions, high pH, and the formation of loose floc are likely to preclude these materials from conventional wastewater treatments. However, CCF are potentially suitable for incorporation into permeable reactive barriers for the containment of metal species in contaminated groundwaters, sediments, and soils.

Author Contributions: Conceptualization, N.J.C.; methodology, N.J.C.; software, N.J.C.; validation, N.J.C. and A.P.H.; formal analysis, N.J.C., A.P.H. and A.A.C.; investigation, N.J.C. and A.P.H.; resources, N.J.C.; data curation, N.J.C.; writing—original draft preparation, N.J.C.; writing—review and editing, A.P.H. and A.A.C.; visualization, N.J.C.; supervision, N.J.C.; project administration, N.J.C.; funding acquisition, N.J.C. All authors have read and agreed to the published version of the manuscript.

Funding: This research received no external funding.

Institutional Review Board Statement: Not applicable.

Informed Consent Statement: Not applicable.

Data Availability Statement: Raw data are available from the corresponding author on request.

Acknowledgments: The authors gratefully acknowledge the technical support of Ian Slipper and Christine Dimech for the collection of the SEM and EDX data.

Conflicts of Interest: The authors declare no conflict of interest.

References

1. Zimbili, O.; Salim, W.; Ndambuki, M. A review on the usage of ceramic wastes in concrete production. *Int. J. Civil Archit. Struct. Constr. Eng.* **2014**, *8*, 91–95.
2. Meng, T.; Hong, Y.; Ying, K.; Wang, Z. Comparison of technical properties of cement pastes with different activated recycled powder from construction and demolition waste. *Cem. Concr. Compos.* **2021**, *120*, 104065. [CrossRef]
3. Gálvez-Martos, J.-L.; Styles, D.; Schoenberger, H.; Zeschmar-Lahl, B. Construction and demolition waste best management practice in Europe. *Resour. Conserv. Recycl.* **2018**, *136*, 166–178. [CrossRef]
4. Huang, B.; Wang, X.; Kua, H.; Geng, Y.; Bleischwitz, R.; Ren, J. Construction and demolition waste management in China through the 3R principle. *Resour. Conserv. Recycl.* **2018**, *129*, 36–44. [CrossRef]
5. Ma, Z.; Li, J.-S.; Xue, Q.; Zhan, B.; Chen, X.; Wan, Y.; Zhao, Y.; Sun, Y.; Poon, C.S. Deep insight on mechanism and contribution of As(V) removal by thermal modification waste concrete powder. *Sci. Total Environ.* **2022**, *807*, 150764. [CrossRef]
6. Gartner, E.M.; Young, J.F.; Damidot, D.A.; Jawed, I. Hydration of Portland cement. In *Structure and Performance of Cements*, 2nd ed.; Bensted, J., Barnes, P., Eds.; Spon Press: London, UK, 2002; pp. 57–113.
7. Conner, J.R.; Hoeffner, S.L. The history of stabilization/solidification technology. *Crit. Rev. Environ. Sci. Technol.* **1998**, *28*, 325–396. [CrossRef]
8. Evans, N.D.M. Binding mechanisms of radionuclides to cement. *Cem. Concr. Res.* **2008**, *38*, 543–553. [CrossRef]
9. Shin, W.-S.; Na, K.-R.; Kim, Y.-K. Adsorption of metal ions from aqueous solution by recycled aggregate: Estimation of pretreatment effect. *Desalin. Water Treat.* **2016**, *57*, 9366–9374. [CrossRef]
10. Damrongsiri, S. Feasibility of using demolition waste as an alternative heavy metal immobilising agent. *J. Environ. Manag.* **2017**, *192*, 197–202. [CrossRef]
11. Kumara, G.M.P.; Kawamoto, K.; Saito, T. Evaluation of autoclaved aerated concrete fines for removal of Cd(II) and Pb(II) from wastewater. *J. Environ. Eng.* **2019**, *145*, 04019078. [CrossRef]
12. Coleman, N.J.; Lee, W.E.; Slipper, I.J. Interactions of aqueous Cu^{2+}, Zn^{2+} and Pb^{2+} ions with crushed concrete fines. *J. Hazard. Mater.* **2005**, *121*, 203–213. [CrossRef] [PubMed]
13. Ali, A.F.; Abd Ali, Z.T. Removal of lead ions from wastewater using crushed concrete demolition waste. *Assoc. Arab Univ. J. Eng. Sci.* **2019**, *26*, 22–29. [CrossRef]
14. Ali, A.F.; Abd Ali, Z.T. Interaction of aqueous Cu^{2+} ions with granules of crushed concrete. *Iraqi J. Chem. Pet. Eng.* **2019**, *20*, 31–38. [CrossRef]
15. Yoo, J.; Shin, H.; Ji, S. Evaluation of the applicability of concrete sludge for the removal of Cu, Pb, and Zn from contaminated aqueous solutions. *Metals* **2018**, *8*, 666. [CrossRef]
16. Deng, Y.; Wheatley, A. Mechanisms of phosphorus removal by recycled crushed concrete. *Int. J. Environ. Res. Public Health* **2018**, *15*, 357. [CrossRef]
17. Jelić, I.; Šljivić-Ivanović, M.; Dimović, S.; Antonijević, D.; Jović, M.; Vujović, Z.; Smičiklas, I. Radionuclide immobilization by sorption onto waste concrete and bricks-experimental design methodology. *Water Air Soil Pollut.* **2019**, *230*, 242. [CrossRef]
18. Šljivić-Ivanović, M.; Ivana, J.; Dimović, S.; Antonijević, D.; Jović, M.; Mraković, A.; Smičiklas, I. Exploring innovative solutions for aged concrete utilization: Treatment of liquid radioactive waste. *Clean Technol. Environ. Policy* **2018**, *20*, 1343–1354. [CrossRef]
19. Jelić, I.; Šljivić-Ivanović, M.; Dimović, S.; Antonijević, D.; Jović, M.; Mirković, M.; Smičiklas, I. The applicability of construction and demolition waste components for radionuclide sorption. *J. Clean. Prod.* **2018**, *171*, 322–332. [CrossRef]
20. Shin, W.-S.; Kim, Y.-K. Removal characteristics of heavy metals from aqueous solution by recycled aggregate and recycled aggregate/steel slag composites as industrial byproducts. *Appl. Chem. Eng.* **2015**, *26*, 477–482. [CrossRef]
21. Liu, C.; Yang, Y.; Wan, N. Kinetic studies of phosphate adsorption onto construction solid waste (CSW). *Water Qual. Res. J. Can.* **2014**, *49*, 307–318. [CrossRef]

22. Egemose, S.; Sønderup, M.J.; Beinthin, M.V.; Reitzel, K.; Hoffmann, C.C.; Flindt, M.R. Crushed concrete as a phosphate binding material: A potential new management tool. *J. Environ. Qual.* **2012**, *41*, 647–653. [CrossRef] [PubMed]
23. Wu, L.; Tang, J.; Zhang, S.; Wang, J.; Ding, X. Using recycled concrete as an adsorbent to remove phosphate from polluted water. *J. Environ. Qual.* **2019**, *48*, 1489–1497. [CrossRef] [PubMed]
24. dos Reis, G.S.; Cazacliu, B.G.; Corread, C.R.; Ovsyannikovad, E.; Krused, A.; Sampaio, C.H.; Lima, E.C.; Dotto, G.L. Adsorption and recovery of phosphate from aqueous solution by the construction and demolition wastes sludge and its potential use as phosphate-based fertilizer. *J. Environ. Chem. Eng.* **2020**, *8*, 103605. [CrossRef]
25. Kittnerová, J.; Drtinová, B.; Štamberg, K.; Vopálka, D.; Evans, N.; Deissmann, G.; Lange, S. Comparative study of radium and strontium behaviour in contact with cementitious materials. *Appl. Geochem.* **2020**, *122*, 104713. [CrossRef]
26. Wieland, E.; Tits, J.; Kunz, D.; Dähn, R. Strontium uptake by cementitious materials. *Environ. Sci. Technol.* **2008**, *42*, 403–409. [CrossRef]
27. Tumolo, M.; Ancona, V.; De Paola, D.; Losacco, D.; Campanale, C.; Massarelli, C.; Uricchio, V.F. Chromium pollution in European water, sources, health risk, and remediation strategies: An overview. *Int. J. Environ. Res. Public Health* **2020**, *17*, 5438. [CrossRef]
28. Vincent, J.B. New Evidence against chromium as an essential trace element. *J. Nutr.* **2017**, *147*, 2212–2219. [CrossRef]
29. Pavesi, T.; Moreira, J.C. Mechanisms and individuality in chromium toxicity in humans. *J. Appl. Toxicol.* **2020**, *40*, 1183–1197. [CrossRef]
30. Moulin, I.; Rosea, J.; Stone, W.; Bottero, J.-Y.; Mosnier, F.; Haelmel, C. Lead, zinc and chromium (III) and (VI) speciation in hydrated cement phases. In *Waste Materials in Construction*; Woolley, G.R., Goumans, J.J.J.M., Wainwright, P.J., Eds.; Elsevier: Oxford, UK, 2000; Volume 1, pp. 269–280.
31. Johnson, D.C.; Coleman, N.J.; Lane, J.; Hills, C.D.; Poole, A.B. A preliminary investigation of the removal of heavy metal species from aqueous media using crushed concrete fines. In *Waste Materials in Construction*; Woolley, G.R., Goumans, J.J.J.M., Wainwright, P.J., Eds.; Elsevier: Oxford, UK, 2000; Volume 1, pp. 1044–1049.
32. Genchi, G.; Carocci, A.; Lauria, G.; Sinicropi, M.S.; Catalano, A. Nickel: Human health and environmental toxicology. *Int. J. Environ. Res. Public Health* **2020**, *17*, 679. [CrossRef]
33. Colarusso, P.; Guo, B.; Zhang, K.-Q.; Bernath, P.F. High-resolution infrared emission spectrum of strontium monofluoride. *J. Mol. Spectrosc.* **1996**, *175*, 158–171. [CrossRef]
34. Zamburlini, M.; Campbell, J.L.; de Silveira, G.; Butler, R.; Pejović-Milić, A.; Chettle, D.R. Strontium depth distribution in human bone measured by micro-PIXE. *X-ray Spectrom.* **2009**, *38*, 271–277. [CrossRef]
35. Emsley, J. *Nature's Building Blocks: An A-Z Guide to the Elements*, 2nd ed.; Oxford University Press: New York, NY, USA, 2011.
36. Iwaida, T.; Nagasaki, S.; Tanaka, S. Sorption study of strontium onto hydrated cement phases using a sequential desorption method. *Radiochim. Acta* **2000**, *88*, 483–486. [CrossRef]
37. Elmes, V.K.; Coleman, N.J. Interactions of Cd^{2+}, Co^{2+} and MoO_4^{2-} ions with crushed concrete fines. *J. Compos. Sci.* **2021**, *5*, 42. [CrossRef]
38. Azizian, S. Kinetic models of sorption: A theoretical analysis. *J. Colloid Interface Sci.* **2004**, *276*, 47–52. [CrossRef]
39. Yarusova, S.B.; Gordienko, P.S.; Yudakov, A.A.; Azarova, Y.A.; Yashchuk, R.D. Kinetics of the sorption of heavy-metal ions by a sorbent obtained from boric acid production waste. *Theor. Found Chem. Eng.* **2016**, *50*, 841–845. [CrossRef]
40. Ho, Y.S.; McKay, G. Pseudo-second order model for sorption processes. *Process Biochem.* **1999**, *34*, 451–465. [CrossRef]
41. Cheng, T.W.; Lee, M.L.; Ko, M.S.; Ueng, T.H.; Yang, S.F. The heavy metal adsorption characteristics on metakaolin-based geopolymer. *Appl. Clay Sci.* **2012**, *56*, 90–96. [CrossRef]
42. Zou, J.; Guo, C.; Zhou, X.; Sun, Y.; Yang, Z. Sorption capacity and mechanism of Cr^{3+} on tobermorite derived from fly ash acid residue and carbide slag. *Colloids Surf. A* **2018**, *538*, 825–833. [CrossRef]
43. Niuniavaite, D.; Baltakys, K.; Dambrauskas, T.; Eisinas, A. Cu^{2+}, Co^{2+} and Cr^{3+} adsorption by synthetic dibasic calcium silicate hydrates and their thermal stability in a 25–1000 °C temperature range. *J. Therm. Anal. Calorim.* **2019**, *138*, 2241–2249. [CrossRef]
44. Ghorbel-Abid, I.; Jrad, A.; Nahdi, K.; Trabelsi-Ayadi, M. Sorption of chromium (III) from aqueous solution using bentonitic clay. *Desalination* **2009**, *246*, 595–604. [CrossRef]
45. Flieger, J.; Kawka, J.; Płaziński, W.; Panek, R.; Madej, J. Sorption of heavy metal ions of chromium, manganese, selenium, nickel, cobalt, iron from aqueous acidic solutions in batch and dynamic conditions on natural and synthetic aluminosilicate sorbents. *Materials* **2020**, *13*, 5271. [CrossRef] [PubMed]
46. Ali, A.F.; Abd Ali, Z.T. Sustainable use of concrete demolition waste as reactive material in permeable barrier for remediation of groundwater: Batch and continuous study. *J. Environ. Eng.* **2020**, *146*, 04020048. [CrossRef]
47. Jelić, I.; Šljivić-Ivanović, M.; Dimović, S.; Antonijević, D.; Jović, M.; Šerović, R.; Smičiklas, I. Utilization of waste ceramics and roof tiles for radionuclide sorption. *Process Saf. Environ. Protect.* **2017**, *105*, 348–360. [CrossRef]
48. Coleman, N.J.; Brassington, D.S.; Raza, A.; Mendham, A.P. Sorption of Co^{2+} and Sr^{2+} by waste-derived 11 Å tobermorite. *Waste Manag.* **2006**, *26*, 260–267. [CrossRef] [PubMed]
49. Huang, Y.-H.; Wu, Y.-C. Highly efficient adsorption of Sr^{2+} and Co^{2+} ions by ambient prepared alkali activated metakaolin. *Polymers* **2022**, *14*, 992. [CrossRef] [PubMed]
50. Rumble, J. (Ed.) *CRC Handbook of Chemistry and Physics*, 99th ed.; CRC Press: Boca Raton, FL, USA, 2018; pp. 5–189. ISBN 1138561630.

51. Regmi, G.; Indraratna, B.; Nghiem, L.D.; Golab, A.; Prasad, B.G. Treatment of acid groundwater in acid sulphate soil terrain using recycled concrete: Column experiments. *J. Environ. Eng.* **2011**, *137*, 433–443. [CrossRef]
52. Banasiak, L.; Indraratna, B.; Regmi, G.; Golab, A.; Lugg, G. Characterisation and assessment of recycled concrete aggregates used in a permeable reactive barrier for the treatment of acidic groundwater. *Geomech. Geoengin.* **2013**, *8*, 155–166. [CrossRef]
53. Banasiak, L.B.; Indraratna, B.; Lugg, G.; Pathirage, U.; McIntosh, G.; Rendell, N. Permeable reactive barrier rejuvenation by alkaline wastewater. *Environ. Geotech.* **2015**, *2*, 45–55. [CrossRef]
54. Medawela, S.; Indraratna, B.; Athuraliya, S.; Lugg, G.; Nghiem, L.D. Monitoring the performance of permeable reactive barriers constructed in acid sulfate soils. *Eng. Geol.* **2022**, *296*, 106465. [CrossRef]